Journal of Peptide Science
J. Peptide Sci. **9**: 714–728 (2003)
Published online in Wiley InterScience (www.interscience.wiley.com). DOI: 10.1002/psc.459

JOURNAL OF PEPTIDE SCIENCE

Circular Dichroism Studies of Ampullosporin-A Analogues‡

HOAI-HUONG NGUYEN,[a] DIANA IMHOF,[a] MATTHIAS KRONEN,[b] UDO GRÄFE[b§] and SIEGMUND REISSMANN[a]*

[a] Institut für Biochemie und Biophysik, Friedrich-Schiller-Universität Jena, Philosophenweg 12, D-07743 Jena, Germany
[b] Hans-Knöll-Institut für Naturstoffforschung, Beutenbergstraße 11, D-07745 Jena, Germany

Received 3 July 2002
Accepted 16 December 2002

Abstract: Ampullosporin A (AmpA), a 15mer peptaibol containing seven Aib residues is able to induce pigmentation on *Phoma destructiva* and hypothermia in mice, as well as to exhibit a neuroleptic effect. A circular dichroism study of ampullosporin A and its analogues was carried out in organic solvents with different polarities and detergent micelles to determine the relationship between their conformational flexibility and biological activities. The analogues were obtained by modifying the *N*- and *C*-termini of ampullosporin A. Furthermore, Gln and Leu were systematically substituted by Ala and Aib residues were replaced by Ala and/or Ac_6c. To estimate the helicity of the analogues, the CD spectrum of AmpA recorded in acetonitrile was correlated to its crystal structure. All analogues displayed similar CD curve shapes in organic solvents with the ratio between two negative band intensities $R = [\theta]_{n-\pi^*}/[\theta]_{\pi-\pi^*} < 1$. In acetonitrile, most of the analogues adopted a 70%–85% helical structure, which was higher than the average of 40%–60% obtained in TFE. In detergent micelles, the analogues were distinguishable by their CD profiles. For most of the biologically active analogues, the CD spectra in detergent micelles were characterized by a R ratio > 1 and increased helicity compared with those recorded in TFE, suggesting that the interaction of the peptides with the membrane and peptide association was necessary for their hypothermic effect.

Keywords: peptaibol; conformational study; circular dichroism

INTRODUCTION

A number of natural ampullosporin analogues: ampullosporin A (AmpA), ampullosporin B (AmpB), ampullosporin C (AmpC) and ampullosporin D (AmpD) have been isolated from the fungus *Sepedonium ampullosporum* [1,2]. They belong to the peptaibol class of natural products, characterized by the presence of an acetylated *N*-terminus, a *C*-terminal amino alcohol and a high proportion of α-aminoisobutyric acid (Aib). Peptaibols were reported to exhibit membrane permeabilizing activity [3–5]. For instance, alamethicin [5] and chrysospermin [6] can form ion channels, whereas antiamoebin [7] acts as an ion carrier and trichogin [8] induces the leakage of aqueous content from liposomes. Ampullosporins, strongly

Abbreviations: Abbreviations used for amino acids follow the Recommendations of the IUPAC-IUB Biochemical Nomenclature (*Eur. J. Biochem.* 1984; **138**: 9–37). The following additional abbreviations are used throughout the text: Ac_6c, 1-amino-1-cyclohexane carboxylic acid; AmpA (B, C, D), ampullosporin A (B, C, D); CD, circular dichroism; CMC, critical micellar concentration; DPC, dodecyl phosphocholine; EtOH, ethanol; HFIP, 1,1,1,3,3,3-hexafluoroisopropanol; iPrOH, isopropanol; MeOH, methanol; MeCN, acetonitrile; MRE, mean residue ellipticity; NMR, nuclear magnetic resonance; Oic, octahydro-1H-indole-2-carboxylic acid; SDS, sodium dodecylsulphate; TFE, 2,2,2-trifluoroethanol; Tic, 1,2,3,4-tetrahydroisoquinoline-3-carboxylic acid.

*Correspondence to: Professor Siegmund Reissmann, Institut für Biochemie und Biophysik, Friedrich-Schiller-Universität Jena, Philosophenweg 12, D-07743 Jena, Germany;
e-mail: reissmann@merlin.biologie.uni-jena.de
‡ Presented at Peptaibols, October 2002, Jena, Germany.
§ Deceased.
Contract/grant sponsor: Deutsche Forschungsgemeinschaft; Contract/grant number: 853/7-1.

hydrophobic and devoid of charges, are also believed to have a site of action in the membrane. The Trp residue at the *N*-terminus may interact with the bilayer interface as a membrane anchor [9,10]. The membrane conductance as a function of natural ampullosporin concentration showed the formation of ion conducting pores in the artificial bilayer [11,12].

The conformation of AmpA, solved by x-ray diffraction, is a largely regular α-helix starting from the acetylated *N*-terminus and a β-turn at the *C*-terminus [13]. In similarity to alamethicin [14] and chrysospermin [6], AmpA helices possess a hydrophilic face formed by the polar side chains of Gln^{7}, Gln^{11}, and non hydrogen bonding carbonyl oxygens of Aib^{10} and Gln^{11}, while the hydrophobic face is formed by the bulky side chains of Trp^{1}, Leu^{5}, Leu^{12} and Leu^{15}ol. The length of AmpA in the crystals is only 23 Å, much shorter than that of antiamoebin (28.3 Å), a 16mer peptaibol [7]. Compared with the core thickness of the bilayer, which varies from 19.5 Å to 29 Å [5], a single molecule of AmpA hardly spans the standard bilayer even when it produces a membrane thinning effect. On the other hand, the crystal packing of AmpA shows its ability to self-associate via hydrogen bonds in a head-to-tail fashion and in antiparallel fashion due to polar side chains and the non hydrogen bonding carbonyl oxygen of Aib^{10} [13]. If this hydrogen bonding can also occur in the membrane, the pore forming activity of AmpA might be explained according to the barrel-stave model by the flip-flop mechanism [15]. However, in contrast to alamethicin, AmpA displayed only a weak antimicrobial effect [1]. The more interesting biological activity of AmpA and its natural analogues is related to their ability to induce pigment formation in the fungus *Phoma destructiva*, as do several commercial nonpeptide antipsychotics haloperidol, chlorpromazine, clozapine and sertindole [1,2]. In addition, natural ampullosporins can also provoke hypothermia and inhibit locomotor activity in mice [1,2]. Specific behavioural tests confirmed the assumption of an atypical neuroleptic activity of AmpA [16].

Whereas the biological activities of peptaibols, such as antimicrobial, antimalarial and haemolytic activities, stimulation of catecholamine secretion, uncouplers of mitochondrial oxidative phosphorylation [3,4] etc. were reported to be generated from their membrane activities, the action mechanisms of the biological activities of ampullosporins remain unknown. To elucidate the relationship between the conformation and biological activities of ampullosporins, a set of AmpA analogues has been synthesized by solid phase peptide synthesis and their biological activities have been tested [17]. The analogues are different in their *C*- and *N*-termini and also in the number of Aib residues. Some analogues retain as high pigment induction activity and as strong hypothermic effect as AmpA whereas others exhibit strong pigment induction activity together with a significantly reduced hypothermic response. Analogues without aromatic residues or 14mer analogues are devoid of any biological activity. Furthermore, the acetylated *N*-terminus and hydroxylated or amidated *C*-terminus seem to play an important role in the hypothermic activity, too. The replacement of Aib residues by Ala or Ac_6c (see Abbreviations) at different sequence positions affected likewise the biological activities. To check the effect of side chains on biological activities of ampullosporin analogues, Gln and Leu residues were individually substituted by Ala. Whereas replacement of every Gln by Ala did not affect the biological activities, the lack of a Leu side chain led to a loss of pigment induction and to a reduction of hypothermic response.

In the present paper, we report the results of a conformational study of natural and synthetic ampullosporin analogues, using circular dichroism. Circular dichroism is a valuable tool for estimating the secondary structure of proteins and peptides in solution, especially for analysing their conformational change in different environments. To examine the conformation of the peptide in the membranes, detergent micelles SDS and DPC were used, which are considered as membrane mimetic solvents with hydrophobic and hydrophilic interface and which do not distort the spectra from differential light scattering and differential absorption flattening [18]. There are many methods for secondary structure analysis from CD spectra. However, the accuracy of the estimation depends strongly on the reference protein set [19]. Since AmpA and most of its analogues contain nearly 50% of achiral Aib residues, the use of references from proteins and polypeptides containing usual amino acids is not appropriate. In this study, the helical content of the analogues was determined at a single wavelength of about 222 nm with reference data taken from the crystal structure of AmpA.

MATERIALS AND METHODS

Natural AmpB and AmpD were isolated from *Sepedonium ampullosporum* HKI-0053 [2]. AmpA,

Table 1 Ampullosporin A Analogues

Peptide	Modification	Sequence
AmpA	Native	Ac-Trp^{1}-Ala^{2}-Aib^{3}-Aib^{4}-Leu^{5}-Aib^{6}-Gln^{7}-Aib^{8}-Aib^{9}-Aib^{10}-Gln^{11}-Leu^{12}-Aib^{13}-Gln^{14}-Leu^{15}ol
1	[des-Ac]AmpA	**H**-Trp^{1}-Ala^{2}-Aib^{3}-Aib^{4}-Leu^{5}-Aib^{6}-Gln^{7}-Aib^{8}-Aib^{9}-Aib^{10}-Gln^{11}-Leu^{12}-Aib^{13}-Gln^{14}-Leu^{15}ol
2	[des-Trp^{1}]AmpA	**Ac-Ala^{2}**-Aib^{3}-Aib^{4}-Leu^{5}-Aib^{6}-Gln^{7}-Aib^{8}-Aib^{9}-Aib^{10}-Gln^{11}-Leu^{12}-Aib^{13}-Gln^{14}-Leu^{15}ol
3	[D-Trp^{1}]AmpA	Ac-**D-Trp^{1}**-Ala^{2}-Aib^{3}-Aib^{4}-Leu^{5}-Aib^{6}-Gln^{7}-Aib^{8}-Aib^{9}-Aib^{10}-Gln^{11}-Leu^{12}-Aib^{13}-Gln^{14}-Leu^{15}ol
4	[Tic^{1}]AmpA	Ac-**Tic^{1}**-Ala^{2}-Aib^{3}-Aib^{4}-Leu^{5}-Aib^{6}-Gln^{7}-Aib^{8}-Aib^{9}-Aib^{10}-Gln^{11}-Leu^{12}-Aib^{13}-Gln^{14}-Leu^{15}ol
5	[Oic^{1}]AmpA	Ac-**Oic^{1}**-Ala^{2}-Aib^{3}-Aib^{4}-Leu^{5}-Aib^{6}-Gln^{7}-Aib^{8}-Aib^{9}-Aib^{10}-Gln^{11}-Leu^{12}-Aib^{13}-Gln^{14}-Leu^{15}ol
6	[Leu^{15}]AmpA	Ac-Trp^{1}-Ala^{2}-Aib^{3}-Aib^{4}-Leu^{5}-Aib^{6}-Gln^{7}-Aib^{8}-Aib^{9}-Aib^{10}-Gln^{11}-Leu^{12}-Aib^{13}-Gln^{14}**-Leu^{15}**
7	[des-Leu^{15}ol, Gln^{14}]AmpA	Ac-Trp^{1}-Ala^{2}-Aib^{3}-Aib^{4}-Leu^{5}-Aib^{6}-Gln^{7}-Aib^{8}-Aib^{9}-Aib^{10}-Gln^{11}-Leu^{12}-Aib^{13}**-Gln^{14}**
8	[Leu^{15}-NH$_2$]AmpA	Ac-Trp^{1}-Ala^{2}-Aib^{3}-Aib^{4}-Leu^{5}-Aib^{6}-Gln^{7}-Aib^{8}-Aib^{9}-Aib^{10}-Gln^{11}-Leu^{12}-Aib^{13}-Gln^{14}**-Leu^{15}-NH$_2$**
9	[Ala^{15}-NH$_2$]AmpA	Ac-Trp^{1}-Ala^{2}-Aib^{3}-Aib^{4}-Leu^{5}-Aib^{6}-Gln^{7}-Aib^{8}-Aib^{9}-Aib^{10}-Gln^{11}-Leu^{12}-Aib^{13}-Gln^{14}**-Ala^{15}-NH$_2$**
10	[Ala^{12}]AmpA	Ac-Trp^{1}-Ala^{2}-Aib^{3}-Aib^{4}-Leu^{5}-Aib^{6}-Gln^{7}-Aib^{8}-Aib^{9}-Aib^{10}-Gln^{11}**-Ala^{12}**-Aib^{13}-Gln^{14}-Leu^{15}ol
11	[Ala^{5}]AmpA	Ac-Trp^{1}-Ala^{2}-Aib^{3}-Aib^{4}**-Ala^{5}**-Aib^{6}-Gln^{7}-Aib^{8}-Aib^{9}-Aib^{10}-Gln^{11}-Leu^{12}-Aib^{13}-Gln^{14}-Leu^{15}ol
12	[Ala^{14}]AmpA	Ac-Trp^{1}-Ala^{2}-Aib^{3}-Aib^{4}-Leu^{5}-Aib^{6}-Gln^{7}-Aib^{8}-Aib^{9}-Aib^{10}-Gln^{11}-Leu^{12}-Aib^{13}**-Ala^{14}**-Leu^{15}ol
13	[Ala^{11}]AmpA	Ac-Trp^{1}-Ala^{2}-Aib^{3}-Aib^{4}-Leu^{5}-Aib^{6}-Gln^{7}-Aib^{8}-Aib^{9}-Aib^{10}**-Ala^{11}**-Leu^{12}-Aib^{13}-Gln^{14}-Leu^{15}ol
14	[Ala^{7}]AmpA	Ac-Trp^{1}-Ala^{2}-Aib^{3}-Aib^{4}-Leu^{5}-Aib^{6}**-Ala^{7}**-Aib^{8}-Aib^{9}-Aib^{10}-Gln^{11}-Leu^{12}-Aib^{13}-Gln^{14}-Leu^{15}ol
15	[Ala^{3}]AmpA	Ac-Trp^{1}-Ala^{2}**-Ala^{3}**-Aib^{4}-Leu^{5}-Aib^{6}-Gln^{7}-Aib^{8}-Aib^{9}-Aib^{10}-Gln^{11}-Leu^{12}-Aib^{13}-Gln^{14}-Leu^{15}ol
16	[Ala^{4}]AmpA	Ac-Trp^{1}-Ala^{2}-Aib^{3}**-Ala^{4}**-Leu^{5}-Aib^{6}-Gln^{7}-Aib^{8}-Aib^{9}-Aib^{10}-Gln^{11}-Leu^{12}-Aib^{13}-Gln^{14}-Leu^{15}ol
17	[Ala^{6}]AmpA	Ac-Trp^{1}-Ala^{2}-Aib^{3}-Aib^{4}-Leu^{5}**-Ala^{6}**-Gln^{7}-Aib^{8}-Aib^{9}-Aib^{10}-Gln^{11}-Leu^{12}-Aib^{13}-Gln^{14}-Leu^{15}ol
AmpB	Native	Ac-Trp^{1}-Ala^{2}-Aib^{3}-Aib^{4}-Leu^{5}-Aib^{6}-Gln^{7}**-Ala^{8}**-Aib^{9}-Aib^{10}-Gln^{11}-Leu^{12}-Aib^{13}-Gln^{14}-Leu^{15}ol
AmpC	Native	Ac-Trp^{1}-Ala^{2}-Aib^{3}-Aib^{4}-Leu^{5}-Aib^{6}-Gln^{7}-Aib^{8}**-Ala^{9}**-Aib^{10}-Gln^{11}-Leu^{12}-Aib^{13}-Gln^{14}-Leu^{15}ol
AmpD	Native	Ac-Trp^{1}-Ala^{2}-Aib^{3}-Aib^{4}-Leu^{5}-Aib^{6}-Gln^{7}-Aib^{8}-Aib^{9}**-Ala^{10}**-Gln^{11}-Leu^{12}-Aib^{13}-Gln^{14}-Leu^{15}ol
18	[Ala^{13}]AmpA	Ac-Trp^{1}-Ala^{2}-Aib^{3}-Aib^{4}-Leu^{5}-Aib^{6}-Gln^{7}-Aib^{8}-Aib^{9}-Aib^{10}-Gln^{11}-Leu^{12}**-Ala^{13}**-Gln^{14}-Leu^{15}ol
19	[(Ala)$_7$]AmpA	Ac-Trp^{1}-Ala^{2}**-Ala^{3}-Ala^{4}**-Leu^{5}**-Ala^{6}**-Gln^{7}**-Ala^{8}-Ala^{9}-Ala^{10}**-Gln^{11}-Leu^{12}**-Ala^{13}**-Gln^{14}-Leu^{15}ol
20	[Ac$_6$c^{4}]AmpA	Ac-Trp^{1}-Ala^{2}-Aib^{3}**-Ac$_6$c^{4}**-Leu^{5}-Aib^{6}-Gln^{7}-Aib^{8}-Aib^{9}-Aib^{10}-Gln^{11}-Leu^{12}-Aib^{13}-Gln^{14}-Leu^{15}ol
21	[Ala^{3,8,13}, Ac$_6$c^{6}]AmpA	Ac-Trp^{1}-Ala^{2}**-Ala^{3}**-Aib^{4}-Leu^{5}**-Ac$_6$c^{6}**-Gln^{7}**-Ala^{8}**-Aib^{9}-Aib^{10}-Gln^{11}-Leu^{12}**-Ala^{13}**-Gln^{14}-Leu^{15}ol
22	[Ala^{3,8,13}, Ac$_6$c^{9}]AmpA	Ac-Trp^{1}-Ala^{2}**-Ala^{3}**-Aib^{4}-Leu^{5}-Aib^{6}-Gln^{7}**-Ala^{8}-Ac$_6$c^{9}**-Aib^{10}-Gln^{11}-Leu^{12}**-Ala^{13}**-Gln^{14}-Leu^{15}ol

AmpC and other analogues were synthesized by solid phase method, using the automated peptide synthesizer ECOSYN P (Eppendorf, Biotronik) (Table 1). Details of the synthesis, cleavage, purification and characterization of the peptides were reported elsewhere [17]. MeOH, EtOH, iPrOH, TFE, HFIP, MeCN (for UV-spectroscopy or GC) were purchased from Fluka (Steinheim, Germany), and Fisher Chemicals (Loughborough, UK), SDS and DPC were from Sigma Aldrich Chemie GmbH (Steinheim, Germany) and Avantipolar Lipids (Alabaster, USA), respectively. CD spectra were recorded using a Jasco model 720 spectropolarimeter (Umstadt, Germany). The optical rotation was calibrated using d-camphorsulphonic acid at 290.5 nm [20]. Unless otherwise stated, measurements of three scans were recorded using rectangular quartz cells of 0.1 cm pathlength, 2 nm bandwidth, 20 nm/min scan speed, 8 s time constant, and at 22 °C. The background spectra were recorded in the same solvent without peptide and then subtracted. The spectra reported here are the average of three experiments. Except for the CD spectra recorded in water, other spectra were obtained with samples prepared from stock solutions of 1 mM peptide in TFE. TFE concentration in samples for CD measurements never exceeded 10% and equivalent concentrations of TFE were added to control samples. In samples containing detergents, phosphate buffer saline pH = 7.4 was added at 10 mM, DPC and SDS concentrations were 20 and 50 mM, respectively. Peptide stock solution concentrations were determined by measuring the absorbance of Trp at 280 nm in 6 M guanidine hydrochloride, 10 mM phosphate buffer saline (PBS), pH = 7.4, using $\varepsilon_{280\ nm} = 5690\ M^{-1}\ cm^{-1}$ [20].

Ellipticity at about 222 nm (n-π^* transition) is assumed to be linearly related to the mean helix content f_H, which can be calculated from the Lifson-Roig based helix-coil model [21]:

$$f_H = ([\theta]_{222} - [\theta]_C)/([\theta_H] - [\theta]_C), \quad (1)$$

where $[\theta]_{222}$, $[\theta]_C$ and $[\theta]_H$ are mean residue ellipticities at about 222 nm of the calculated spectrum, random coil and complete helix, respectively. The latter two quantities are temperature dependent and can be determined as follows [21]:

$$[\theta]_C = 2220 - 53T, \quad (2a)$$

$$[\theta]_H = (-44000 + 250T)(1-3/Nr), \quad (2b)$$

where T is temperature in °C, and Nr is the chain length in residues. At 22 °C, $[\theta]_C = 1054$ deg cm^2 dmol^{-1} and $[\theta]_H = -30800$ deg cm^{2}dmol^{-1} for 15mer peptides containing usual amino acids.

The mean helix content f_H can also be obtained by averaging the hydrogen bond probabilities of all residues which can hydrogen bond:

$$f_H = n_H/(Nr - 3), \quad (3)$$

where n_H is the average number of helical hydrogen bonds and (Nr-3) is the number of hydrogen bonds possible in a peptaibol.

RESULTS AND DISCUSSION

CD Spectra of AmpA

Comparison of CD spectra of AmpA in water and different organic solvents. To correlate the CD spectra of AmpA with its crystal structure (Figure 1), CD spectra of AmpA were recorded in a series of organic solvents, including TFE, HFIP, MeOH, EtOH, iPrOH, as well as MeCN, from which the crystals were obtained [13]. Alcohols, particularly TFE and HFIP, have been reported to effectively induce helical structure over other alcohols due to hydrophobic interactions of the solvent molecules and hydrophobic groups of the peptides [22,23]. However, according to Reichardt's overall solvation ability concept (termed also 'polarity', which is measured using the Dimroth-Reichardt's parameter $E_T(30)$ [24]), HFIP and TFE as well as water are strongly polar and MeCN expresses only medium polarity. In alcohols, AmpA is soluble, while in MeCN, it is totally soluble only with the addition of approximately 40% water. However, AmpA crystals were obtained from MeCN with the presence of traces of water. To obtain a concentration independent CD spectrum of AmpA in an MeCN rich environment, 10% TFE was used as a cosolvent.

The CD spectra of AmpA in different solvents are given in Figure 2. With seven Aib, three Leu and one Trp residues, AmpA is very hydrophobic, and hence, its CD spectrum in water is concentration dependent. At a concentration >40 μM, one negative peak at about 205 nm and one positive peak near 194 nm were recorded, while at a lower concentration, the negative peak shifted to 203 nm and the positive peak became negative, suggesting a high random coil content at the lower concentration (data not shown).

The CD spectra of AmpA in MeOH, EtOH, iPrOH and MeCN possessing two pronounced negative

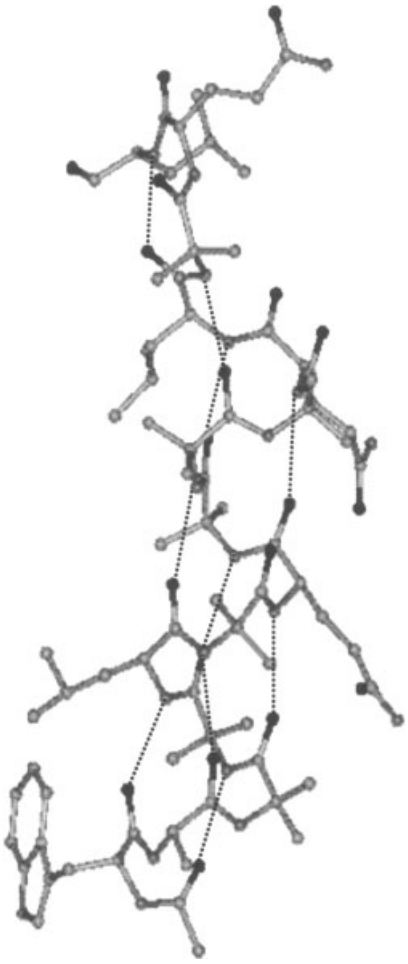

Figure 1 Crystal structure of AmpA, dot lines: hydrogen bonds.

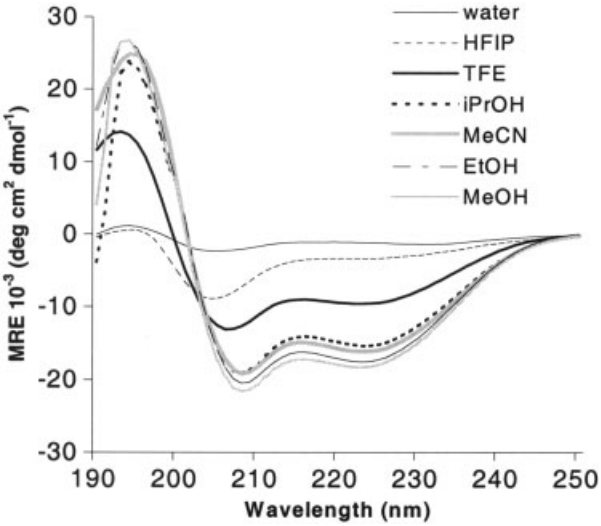

Figure 2 CD spectra of AmpA in water, HFIP, TFE, iPrOH, MeCN, EtOH and MeOH from the top to bottom at 222 nm, peptide concentrations were 86 μM.

minima at 223 nm and 208 nm and a positive maximum near 194 nm are typical for α-helix. These spectra were comparable not only in curve shapes, but also in band magnitudes. Interestingly, the CD spectrum of AmpA in TFE resembled the waveform of those in the above described organic solvents with the following differences: the π-$\pi^*\|$ transition shifted to 206 nm and the intensities of all peaks were significantly reduced. Furthermore, the CD spectrum in HFIP showed one negative peak at 204 nm and a very weak positive peak at about 194 nm. It is likely that the random coil content increased when TFE and especially HFIP were used as solvents. Besides, AmpA is rich in Aib, which have been reported to promote the onset of 3_{10}-helix due to steric interactions involving the *gem*-methyl groups linked to the α-carbon [25]. In Aib containing peptides, the 3_{10}-geometry is energetically favoured over the α-geometry. Therefore, Aib containing peptides adopt pure 3_{10}-, pure α-, or mixed 3_{10}-/α-helices depending on their length and the relative Aib content. In peptides of eight or more residues, a pure α-helix was observed if the Aib content did not exceed 50% [25]. In the crystal structure of AmpA, an α-helical segment from CO of acetyl group to NH of Aib^9 was found (Figure 1). However, several weak hydrogen bonds of type i, $i+3$ were present concomitantly with α-helical hydrogen bonds in the middle of the molecule [13]. The theoretical CD spectrum of 3_{10}-helix calculated by Manning and Woody [26] agreed well with Toniolo's measurements [27], which showed that the right-handed 3_{10}-helical peptide displayed a negative CD band at 207 nm accompanied by a shoulder centred near 222 nm, and the ratio $R = [\theta]_{222}/[\theta]_{207}$ of 0.4. Analysing CD spectra of AmpA in organic solvents, it was found that the R values are 0.83 ± 0.03 in MeOH, EtOH, iPrOH and MeCN, but only 0.73 and 0.36 in TFE and HFIP, respectively. According to [26,27], using the R value to diagnose the presence of a 3_{10}-helix, one can say that in TFE, AmpA adopted a mixture of α- and 3_{10}-helix and in HFIP, the 3_{10}-helical content may be higher. Besides the 3_{10}-helix, other types of β-turn may occur, for example, a β-turn type I. Examining numerous β-turn types [28], it is worth being interested only in β-turn types I and III for AmpA analogues. On the basis of the studies on the CD spectra of β-turn by Woody and Chang [29,30], it was assumed that in TFE and HFIP, the presence of β-turns (including 3_{10}-helix) in different contents

may contribute to a reduction of CD negative band intensities, followed by a blue shift of π-$\pi^*\|$ bands.

To obtain more details on the effect of organic solvents on AmpA secondary structure, AmpA dissolved in water was titrated with TFE (Figure 3). Above 20% TFE, the CD spectra were concentration independent with an isodichroic point at 200 nm. In 50% TFE in water, a spectrum with maximal band intensity was found. There was no difference between the CD spectra in 50% TFE and pure TFE. Interestingly, AmpA in other solvents including HFIP and MeCN containing 50% of water showed CD profiles comparable to those in pure TFE and 50% TFE in water (data not shown). Thus, fluoroalcohols did not induce helical structure of AmpA as effectively as expected and the secondary structure of the peptide in these solvents was quite different from its crystal structure. In contrast, in organic solvents, the CD spectra of AmpA were similar to those of alamethicin and its synthetic analogues, reported by G. Jung's group. The intensities of both Cotton effects were increased in lipophilic solvents and were decreased in strongly polar, hydrogen-bond-forming solvents [31–33].

To ascertain that nothing else except the secondary structure of AmpA (especially no aggregation) was reflected in its CD spectra, the concentration dependence of its CD profiles in organic solvents was studied. The CD spectra of AmpA were found to be concentration independent in TFE, HFIP from

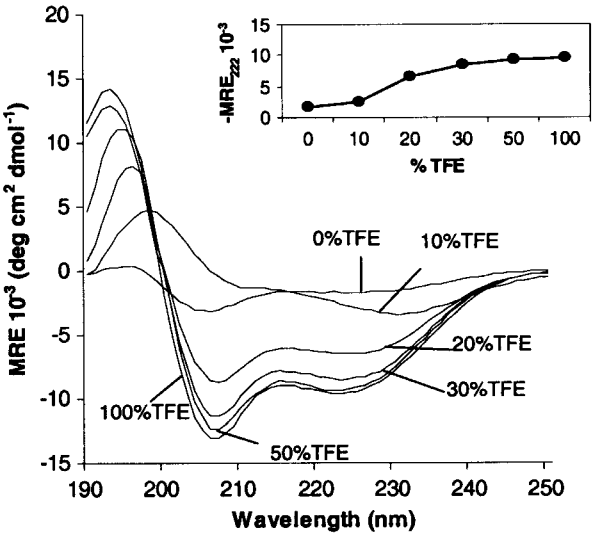

Figure 3 Titration of AmpA with TFE, peptide concentration in the range of 100μM. Inset: MRE_{222} as a function of %TFE.

4 μM to 1 mM and in other alcohols and MeCN (containing 10% TFE) from 4 μM to 100 μM. Therefore, it was assumed that the CD spectrum of AmpA in MeCN (containing 10%TFE) at a concentration <100 μM may correlate with its crystal structure.

Helicity estimation. The crystal structure of AmpA, obtained also from MeCN, contains nine helical hydrogen bonds type i, $i+4$ and one hydrogen bond type i, $i+3$ of β-turn [13]. The mean helical fraction of this 15mer peptaibol calculated using formula (3) is therefore equal to 0.75. Based on formula (1) and $[\theta]_{n-\pi^*}$ of CD spectrum in MeCN, the value of -21840 deg cm^2 dmol^{-1} was obtained for $[\theta]_H$ of AmpA. On the other hand, as has been discussed in Materials and Methods, the quantity $[\theta]_H$ of a 15mer peptide in the absence of Aib residues was equal to $-30\,800$ deg cm^2 dmol^{-1}. The difference between these two ellipticities clearly resulted from the presence of the Aib residues. It is suggested that the average reduced ellipticity caused by each Aib (or any other achiral amino acid) is this difference divided by 7 — the number of the Aib residues in AmpA.

When the number of Aib residues was lower than 7, the data on the crystal structure of the AmpA analogues were not available, and $[\theta]_H$ had to be estimated. Supposing that the AmpA analogue now has n achiral residues, the ellipticity of complete helix is calculated according to

$$[\theta]_H = -21\,840 + [(7-n)(-30\,800 + 21\,840)/7] \text{ deg cm}^2 \text{ dmol}^{-1} \quad (4)$$

Knowing $[\theta]_H$ values, the mean helix contents could be calculated and the average number of helical hydrogen bonds (n_H) of the analogues predicted. In particular, the mean helix content of AmpA analogues was calculated as follows:

$$f_H = ([\theta]_{n-\pi^*} - 1054)/([\theta]_H - 1054) \quad (5)$$

with $[\theta]_H$ being given by formula (4) [cf. formula (1)].

According to this method of helicity calculation, the helical content of AmpA in MeOH, EtOH, iPrOH, MeCN, TFE and HFIP were 85%, 82%, 75%, 75%, 46% and 18% respectively, corresponding to approximately ten helical hydrogen bonds in MeOH and EtOH, nine in MeCN and iPrOH, six in TFE and two in HFIP. The crystal structure of AmpA in MeCN shows that the α-helix from acetyl group to Aib^{13} misses a hydrogen bond between CO of Aib^6 and NH of Aib^{10}. Therefore, the predicted number

of ten helical hydrogen bonds in MeOH and EtOH suggests that in these environments, the peptide may be a regular α-helix from N-acetyl group to Aib[13]. The more flexible region may be at the *C*-terminus, where carbonyl oxygens of Aib[10] and Gln[11] hydrogen bond with other molecule or solvent and Leu[15]ol bonds with Leu[12] to form a β-turn. In TFE, the predicted number of hydrogen bonds being only 6, corresponds to the pure α-helical segment from the carbonyl oxygen of the acetyl group to that of Leu[5]. Aib[6], whose carbonyl oxygen does not form an intramolecular hydrogen bond in the crystal structure, might be the starting position of another structure in TFE.

CD spectrum of AmpA in membrane mimetic solvents. Detergent micelles, providing a simple hydrophobic hydrophilic interface related to the membrane, are considered more representative of the membrane environments than organic solvents [18,34]. Besides SDS, a classical detergent for spectroscopic studies, DPC has been often used for NMR study recently to solve peptaibol structures, because DPC, being a zwitterionic detergent, is expected not to denature the membrane proteins [6,18].

The titration of AmpA with SDS or DPC showed an increase of the positive maximum at 194 nm and negative maxima at 208 nm and 224 nm (Figure 4). An isodichroic point at 202 nm appeared only when detergent was added to some extent. When the peptide totally bound to the detergent micelles (detergent concentrations were higher than critical micellar concentration (CMC)), no change of CD spectra was found upon the detergent addition. Calculated helical fractions of AmpA in SDS and DPC micelles were about 0.65, occupying an intermediate place between those obtained from MeCN and TFE. The difference between the CD spectra in micellar detergents and in organic solvents was in the *R* ratio ($[\theta]_{n-\pi^*}/[\theta]_{\pi-\pi^*}$), which were 0.99 and 1.05 in DPC and SDS, respectively, compared with 0.83 ± 0.03 in MeCN, MeOH, EtOH, and iPrOH, 0.73 in TFE, and 0.36 in HFIP. The *R* values in detergents were even higher in the case without TFE in the CD samples (data not shown). However, all the CD samples contained 10% TFE from the stock solutions, which tended to reduce the peptide interaction, and hence decreased the *R* values. Thus, it is reasonable to state that the CD spectra of AmpA in both SDS and DPC corresponded to those of transmembrane helices (dissolved in buffered detergent), which were characterized by the intensity of the 208 nm band being slightly less negative than that of the 222 nm band [35]. However, the magnitude of the AmpA spectrum was much lower than that of the reported transmembrane helix due to its limited number of amino acids and the large content of achiral Aib residues. In addition, the CD spectra of AmpA in detergent micelles were similar to those of other peptaibols such as alamethicin [31,36–38] and antiamoebin [7] and other models of ion-channels [39] in lipid vesicles. The *R* value >1 is often used to predict helical interactions [31,36,37,39–41]. AmpA with the bulky hydrophobic side chains of Leu and Trp caused hydrophobic interaction in water, which may be disrupted by detergent addition. When the peptide was completely bound to detergent micelles, intermolecular hydrogen bonding of three polar residues Gln may have driven helix association, as demonstrated by Zhou for polyleucine transmembrane helices [42].

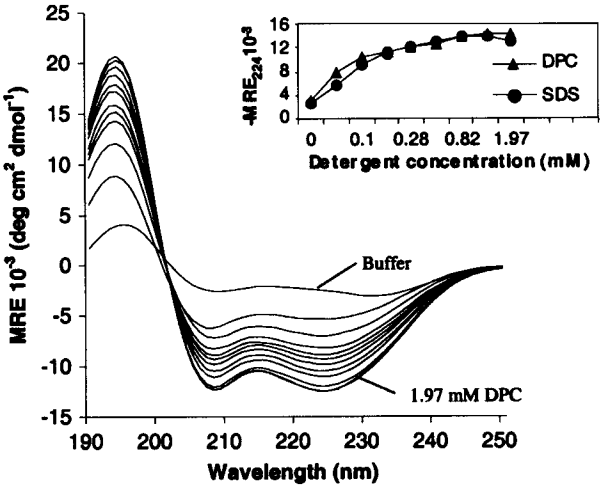

Figure 4 Titration of AmpA with DPC in the range of 0–1.97 mM, peptide concentration 60μM, phosphate buffer saline 10 mM, pH = 7.4. Inset: MRE_{224} as a function of DPC and SDS concentrations.

To obtain more information on the association of AmpA in detergent micelles, the CD spectra were studied at lower concentrations. Figure 5 shows the SDS and DPC titrations to AmpA in the range of 4 μM, the lowest peptide concentration at which the CD could be measured. At first, two negative CD bands grew in intensity upon the increase of SDS concentration up to 0.34 mM. Further SDS addition reduced the 208 nm band and then raised both band intensities again to the maximal values when 1.84 mM SDS was added. When SDS concentration reached 10 mM, both negative peak

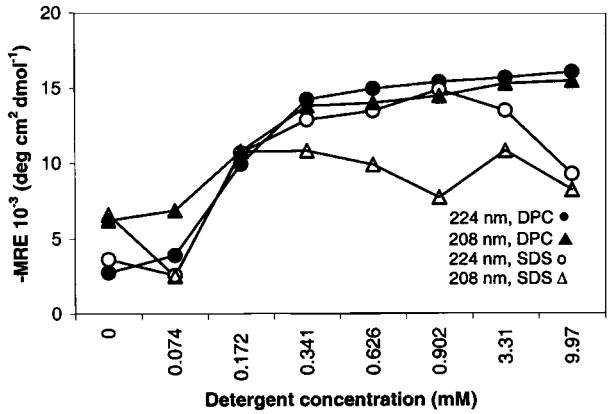

Figure 5 Titration of AmpA with SDS and DPC at low concentration (4μM), phosphate buffer saline 10 mM, pH = 7.4.

intensities were strongly suppressed. This indicates that at low concentration, SDS titration caused some independent state transitions. In contrast, titration of the peptide with DPC in the same range of concentration showed a single isodichroic point at 203 nm and the red-shifted $\pi - \pi^*$ band, indicating a smooth transition from unordered structure to the helical one. Although a certain difference between the titration of high and low concentrations of AmpA with detergents was observed, no clear distinction of their CD spectra in the DPC micelle bound state was found. It is suggested that the peptide association might start at a lower concentration, and thus an appropriate method is necessary to find the critical concentration.

Thermal stability. To better observe the flexibility of AmpA, the thermal stability of its conformation in TFE and SDS was studied (Figure 6). Upon increasing the temperature to 70 °C, a CD spectrum in TFE was obtained with reduced peak intensities. The

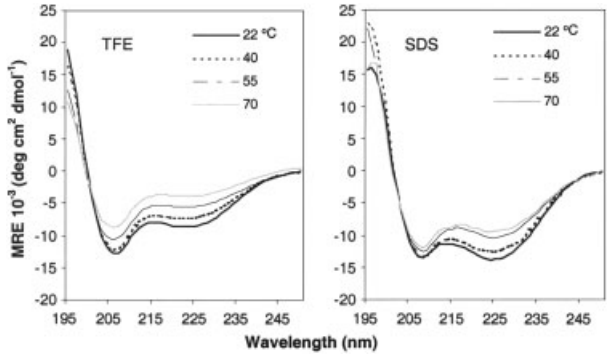

Figure 6 CD spectra of AmpA in TFE and SDS at different temperatures.

R value dropped to 0.43. However, no wavelength shift was found, implying that the change in the CD spectra may be due to the transition of α-helix to 3_{10}-helix or β-turn, but not to unfolding the conformation. Interestingly, heating the AmpA sample in SDS up to the same temperature did not affect its CD spectrum as much as in TFE. The characteristics of helical structure were preserved, in spite of the lower band intensities, especially that around 224 nm, and decreased the *R* value to 0.78. The change in the CD spectra may be contributed by several factors such as fraying ends of α-helices, and/or the diminishment of peptide–SDS micelles interaction.

In summary, the secondary structure of AmpA is very sensitive to change in the environment. The peptide adopts a high helical structure in MeOH, EtOH, iPrOH and MeCN, which is similar to the result of the crystal structure analysis. In more polar solvents such as TFE and HFIP, the helix content decreased, and a 3_{10}-helix or β-turn and an unordered structure may occur. In micellar detergents, the CD spectra were characteristic of helical association with intermediate helicity between MeCN and TFE, implying that the peptide length might be larger than that in the crystals. In this context, TFE may better mimic the membrane interface (highly polar) than the hydrocarbon core (apolar). AmpA molecules form aggregates in water, become monomers accompanied by helix promotion in the interface, and insert into the membrane core with more increased helicity and self-assembly.

CD Spectra of AmpA Analogues

A small modification in the AmpA sequence strongly affected its biological activities [17]. In order to determine whether a single amino acid modification is able to change the peptide conformation, a CD study of some representative analogues in organic solvents, such as MeCN, TFE and micellar SDS and DPC was carried out. For most of the analogues, there was no significant difference in the CD spectra recorded in SDS and DPC.

N-terminal modification. The CD spectra of modified *N*-terminal AmpA analogues (**1,2,** and **5**) are presented in Figure 7. The CD spectrum of [des-Ac]AmpA (**1**) in TFE displayed a negative band at 206 nm, accompanied by a shoulder centred near 228 nm. The ratio *R* was 0.52, suggesting the presence of a high content of 3_{10}-helical structure [27]. Interestingly, the CD spectrum in SDS shifted to

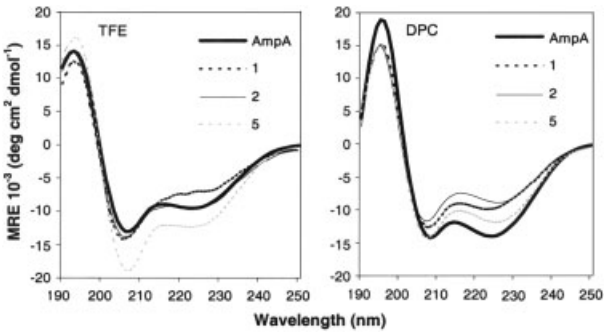

Figure 7 CD spectra of AmpA analogues with modified *N*-terminus.

the higher wavelength but its shape and intensities of all peaks remained the same as in TFE (data not shown). The CD spectrum of the analogue in DPC showed more pronounced band intensity at 224 nm, leading to a higher *R* value (0.78). The calculated helical fractions (see Table 2) in the studied environments were lower than those of AmpA, indicating the role of the acetyl group in the stabilization of the helical structure. The acetyl group is known to be a good *N*-cap of a helix, which encourages α-helix formation at the *N*-terminus and increases the helical content [43,44]. In contrast, Trp is considered a bad *N*-cap (the side chain is in the *gauche*$^+$ rotamer) which is more likely to satisfy its hydrogen bonding potential by forming the alternative *i*, $i+3$ hydrogen bond, equivalent to the formation of 3_{10}-helix [45]. This is consistent with the crystal structure of AmpA, where the acetyl group participates in the α-helix hydrogen bonding, and the side chain of Trp adopts a *gauche*$^+$ rotamer, which certainly favours the formation of a 3_{10}-helix at the *N*-terminus if the acetyl group is removed. Another difference of analogue **1** from AmpA is its particularly thermal stability. Its CD spectrum in SDS was hardly affected by heating up to 70 °C, showing only insignificant change at the 208 nm band intensity (data not shown). This may be explained by the lack of peptide–micelles interaction and the formation of a more stable 3_{10}-helical structure compared with the α-one in Aib containing peptides. Thus, even in detergent micelles, the helicity was not enhanced as much as that of AmpA. Moreover, for both studied detergents, the *R* value was <1, suggesting that no peptide association occurred.

[Des-Trp]AmpA analogue (**2**) displayed CD spectra in TFE and MeCN (see Figure 7 and Table 2) similar in curve shapes to those of AmpA, indicating that the expected contribution of the indole moiety to CD spectra was rather low. Despite being acetylated, the CD spectra of analogue **2** in SDS and DPC preserved a less-than-unity *R* value just as for organic solvents. Moreover, the helical fractions were found to be not more than that in TFE. This suggests that detergent micelles are not a favourable environment for this analogue due to the lack of a hydrophobic residue Trp. The peptide association, therefore, did not occur. Hence, the CD spectra of compounds **1** and **2** indicate an important role of the Trp residue accompanied by an acetyl group at the *N*-terminus of AmpA in the interaction with the detergent micelles, leading to increased helicity and peptide association.

To gain further insight into the role of Trp in the biological activities of AmpA, Trp substituted analogues were synthesized and their conformation investigated. In comparison with the CD spectra of AmpA, those of [D-Trp^1]AmpA (**3**) in TFE and MeCN (Table 2) exhibited similar shapes. However, the spectrum in TFE showed a higher negative band magnitude than that of AmpA, implying a higher helicity, while those of the analogue in detergent micelles showed remarkably low band ellipticities with a red-shifted n-π^* band. The *R* values in SDS and DPC were higher than those in organic solvents, but still much lower than 1. Thus, the orientation of the Trp side chain strongly affects the secondary structure of the peptide, particularly in the membrane mimetic environments.

Another aromatic residue that was incorporated into AmpA instead of L-Trp is Tic (analogue **4**). This residue has neither a flexible side chain like Trp, nor a free HN of the indole group to form a hydrogen bond with the environment. Although the CD spectra of **4** in SDS and DPC displayed $R > 1$, calculated helical fractions of the analogue in all studied environments were lower than those of AmpA (see Table 2).

In analogue **5**, a nonaromatic amino acid Oic replacing Trp increased helicity in MeCN and TFE, but did not affect it in SDS and DPC micelles. However, no clear difference between CD curves shapes in TFE and in detergent micelles were observed, meaning that *R* values were always <1 (see Figure 7 and Table 2). Thus, the lack of an aromatic residue as an interface anchor may lead to the misorientation of the peptide molecules and hence no signal of peptide interaction was seen.

In summary, the *N*-terminus strongly influenced the conformation of the AmpA analogues and at the same time played an important role in their biological activities. The acetyl group favoured a *N*-terminal

Table 2 CD Data and Biological Activities of Ampullosporin A Analogues

Peptide[a]	Modification	Solvent[b]	$[\theta]_{\pi-\pi^*}$	$[\theta]_{n-\pi^*}$	R	f_H	Pigment induction[c]	Hypothermic effect[c]
AmpA	native	MeCN	−19150	−16120	0.84	0.75	**	**
		TFE	−13060	−9540	0.73	0.46		
		DPC	−14220	−14010	0.99	0.66		
1	[des-Ac] AmpA	MeCN	−17640	−12730	0.72	0.60	**	n.a.
		TFE	−14160	−7390	0.52	0.37		
		DPC	−12650	−9890	0.78	0.48		
2	[des-Trp^1] AmpA	MeCN	−18110	−13400	0.74	0.65	n.a.	n.a.
		TFE	−13850	−9700	0.70	0.48		
		DPC	−11770	−8920	0.76	0.45		
3	[D-Trp^1] AmpA	MeCN	−20080	−16330	0.81	0.76	**	*
		TFE	−14810	−11850	0.80	0.56		
		DPC	−12300	−10300	0.84	0.50		
4	[Tic^1] AmpA	MeCN	−13320	−12470	0.94	0.59	**	n.a.
		TFE	−10400	−7880	0.76	0.39		
		DPC	−9300	−10400	1.12	0.50		
5	[Oic^1] AmpA	MeCN	−24800	−21019	0.85	0.96	n.a.	n.a.
		TFE	−18850	−12400	0.66	0.59		
		DPC	−14210	−11900	0.84	0.57		
6	[Leu^{15}] AmpA	MeCN	−20280	−18110	0.89	0.84	**	*
		TFE	−11520	−8910	0.77	0.44		
		DPC	−15250	−15560	1.02	0.73		
7	[des-Leu^{15}ol, Gln^{14}] AmpA	MeCN	−17900	−15890	0.89	0.76	n.a.	n.a.
		TFE	−9640	−7550	0.78	0.39		
		DPC	−13250	−13750	1.04	0.66		
8	[Leu^{15}-NH_2] AmpA	MeCN	−18890	−15340	0.81	0.72	**	**
		TFE	−11590	−7920	0.68	0.39		
		DPC	−14360	−14840	1.03	0.69		
9	[Ala^{15}-NH_2] AmpA	MeCN	−19000	−15840	0.83	0.74	n.a.	*
		TFE	−12230	−8880	0.73	0.43		
		DPC	−16750	−18820	1.12	0.87		
10	[Ala^{12}] AmpA	MeCN	−19930	−16560	0.83	0.77	n.a.	*
		TFE	−12460	−8420	0.68	0.41		
		DPC	−12700	−13110	1.03	0.62		
11	[Ala^5] AmpA	MeCN	−20600	−17410	0.85	0.81	n.a.	*
		TFE	−12370	−8260	0.67	0.41		
		DPC	−14010	−14680	1.05	0.69		
12	[Ala^{14}] AmpA	MeCN	−19780	−15990	0.81	0.74	**	**
		TFE	−11830	−7820	0.66	0.39		
		DPC	−13460	−13800	1.03	0.65		
13	[Ala^{11}] AmpA	MeCN	−19700	−15630	0.79	0.73	**	**
		TFE	−12600	−8330	0.66	0.41		
		DPC	−13580	−13220	0.97	0.62		
14	[Ala^7] AmpA	MeCN	−18620	−14950	0.80	0.70	**	**
		TFE	−11930	−7870	0.66	0.39		
		DPC	−13800	−14340	1.04	0.67		
15	[Ala^3] AmpA	MeCN	−20700	−18440	0.89	0.81	**	**
		TFE	−14300	−12290	0.86	0.55		
		DPC	−14960	−16900	1.13	0.74		

Table 2 (*Continued*)

Peptide[a]	Modification	Solvent[b]	$[\theta]_{\pi-\pi^*}$	$[\theta]_{n-\pi^*}$	*R*	f_H	Pigment induction[c]	Hypothermic effect[c]
16	[Ala^4] AmpA	MeCN	−22020	−18570	0.84	0.81	**	**
		TFE	−14720	−11460	0.78	0.52		
		DPC	−14840	−16050	1.08	0.71		
17	[Ala^6] AmpA	MeCN	−22080	−17800	0.81	0.78	**	n.a.
		TFE	−14520	−9790	0.67	0.45		
		DPC	−15400	−14530	0.94	0.64		
AmpB	native	TFE	−12920	−9690	0.75	0.44	**	**
		SDS	−14630	−14710	1.01	0.65		
AmpC	native	MeCN	−23140	−19230	0.83	0.84	*	*
		TFE	−16660	−12780	0.77	0.57		
		DPC	−16150	−16080	1.00	0.71		
AmpD	native	TFE	−16430	−12150	0.74	0.55	**	**
		SDS	−14770	−15610	1.06	0.69		
18	[Ala^{13}] AmpA	MeCN	−20760	−16070	0.77	0.71	**	**
		TFE	−15140	−9820	0.65	0.45		
		DPC	−14750	−13690	0.93	0.61		
19	[(Ala)$_7$] AmpA	MeCN	−30220	−21980	0.73	0.72	n.a.	n.a.
		TFE	−24960	−18570	0.74	0.62		
		DPC	−24920	−21150	0.85	0.70		
20	[Ac$_6$c^4] AmpA	MeCN	−21340	−18370	0.86	0.85	*	**
		TFE	−12810	−9870	0.77	0.48		
		DPC	−14040	−14590	1.04	0.68		
21	[Ala^{3,8,13}, Ac$_6$c^6] AmpA	MeCN	−22460	−17400	0.77	0.69	*	**
		TFE	−17720	−13210	0.75	0.53		
		DPC	−16160	−14900	0.92	0.60		
22	[Ala^{3,8,13}, Ac$_6$c^9] AmpA	MeCN	−23200	−18930	0.82	0.75	*	**
		TFE	−17880	−14940	0.84	0.60		
		DPC	−17870	−18090	1.01	0.72		

[a] Peptide concentrations were about 100 μM.
[b] DPC, and MeCN samples contain 10% TFE from peptide stock solutions; DPC concentration was 20 mM.
[c] **strong effect, *moderate effect, n.a. no activity [17].

α-helix. The pigment induction was completely lost for analogues containing no aromatic amino acids, whereas the hypothermic response became less pronounced or even disappeared in analogues without the *N*-terminal acetyl group and/or L-Trp. Analogues without Trp or with noncoded Trp related amino acids exhibited considerable change in the CD spectra, accompanied by *R* values <1 or/and reduced helical fractions in detergent micelles. It was therefore assumed that one Trp residue (or at least one aromatic residue) is necessary for anchoring the peptide in the hydrophilic hydrophobic interface, thus determining the precise orientation of the peptide within the membrane. This favours the peptide association in the membranes, leading to (i) their structural stabilization and orientation with respect to a binding membrane protein and (ii) the formation of ion conducting pores. Both mechanisms might be alternatives contributing to the biological activities of AmpA.

C-terminal modifications. Three analogues were synthesized with a modified *C*-terminus (**6,7** and **8**). There were no significant differences in the CD profiles of [Leu^{15}]AmpA (**6**) and [Leu^{15}-NH$_2$] AmpA (**8**), compared with that of AmpA. Analogue **7,** missing one residue, showed lower ellipticities in all environments relative to AmpA, but the helical content was not altered. This *C*-terminal modification, in spite of having no influence on helicity and the *R* value of CD spectra in detergent micelles, affected the biological activities of analogues **6** and **7** [17].

Analogues with modified side chains. Since natural ampullosporins were found to be able to form ion conducting pores in artificial membranes, their biological responses were hypothesized to relate to this activity [11,12]. Although a lipophilic, rigid and helical rod is a sufficient prerequisite for the formation of voltage-gated pores [15], side chains can modulate the amphipathicity and the oligomerization process. Recently, Hara *et al.* [39] studied the side chain effect on the channel activity of Aib rich peptides. According to the authors, peptides with a high degree of helical conformation, high amphipathicity, high affinity for lipid membranes, and self-associating characters in vesicles are the most suitable for inducing ion channels with a high frequency of occurrence. To evaluate the effect of the side chains on the biological activities of AmpA, analogues were synthesized with a systematic replacement of Leu and Gln by Ala.

Compared with analogue **8** (Leu^{15}-NH_2 instead of Leu^{15}ol), the analogue with Ala^{15}-NH_2 (**9**) showed especially higher helical fractions in detergent micelles, leading to an increase of the predicted numbers of helical hydrogen bonds to 11 and *R* values up to 1.12 (see Table 2). The increased *R* values in detergent micelles are a signal of good oligomerization, but the particularly high helicity may render the peptide too short and less flexible. Other analogues (**10** and **11**) with Ala at positions 12 and 5 instead of Leu displayed similar CD spectral properties and they were comparable to those of AmpA. Despite displaying different CD profiles, these three analogues exhibited equivalent biological activities but much weaker than those of AmpA (Figure 8, Table 2).

Interestingly, the systematic substitution of three Gln by Ala did not affect the conformation of the peptides (**12, 13,** and **14**) as much as expected. Spectra in TFE were slightly reduced in peak intensities and *R* values, whereas in detergent micelles, helical fractions were nearly unchanged (see Table 2). In the crystal structure of AmpA, the Gln^{14} side chain, tilting away from the other Gln side chains, forms intermolecular hydrogen bonds with other peptide molecules in a head-to-tail fashion. However, no considerable difference was found in the CD spectra and biological activities between the [Ala^{14}]AmpA analogue (**12**) and AmpA, indicating that the intermolecular hydrogen bond pattern in the solution is different to that in the solid state and dimer formation in the head-to-tail fashion did not exist in AmpA folding under the conditions investigated.

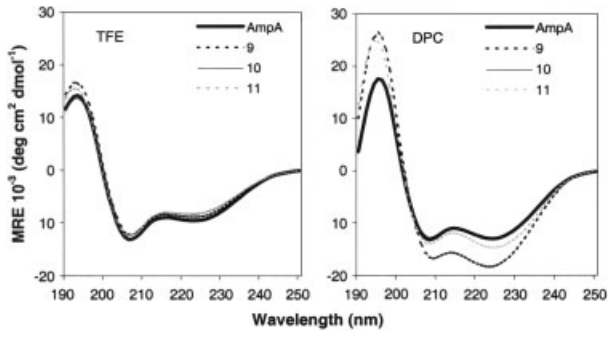

Figure 8 CD spectra of Leu substituted AmpA analogues.

The side chain modification of AmpA did not lead to a great change in the net conformation of analogues, even in the detergent micelles, except for analogue **9** with Ala-NH_2 at the *C*-terminus. The CD profiles for all these analogues suggest their interaction with the detergent micelles. However, it is worth noting that modifications increasing the overall hypophobicity (Gln substituted analogues) seem to favour the biological activities, whereas the less hydrophobic Leu substituted analogues were much less active.

CD spectra of Aib substituted analogues. When all the Aib residues of AmpA were replaced by Ala, analogue **19** was obtained without any biological activity. Analogue **19** is less hydrophobic than AmpA, therefore more soluble in water, showing a high intensity of the CD spectrum in aqueous milieu (data not shown). The analogue displayed much more pronounced CD bands than those of AmpA in all environments due to the chirality of Ala. However, compared with AmpA, **19** adopted a comparable helical structure in MeCN and detergent micelles. It is likely that the helicity of **19** was not as sensitive to the change of environments as AmpA (see Table 2). Furthermore, in spite of possessing a Trp residue, the analogue showed *R* values in micelles only slightly increased relative to those in organic solvents, but always less than 1. This suggests that Aib residues play an important role in the interaction of the peptide with the detergent micelles.

It is interesting that some natural analogues of AmpA, such as AmpB, AmpC and AmpD with Ala at positions 8, 9 and 10 instead of Aib, respectively, were also isolated from the fungal producer of AmpA. In order to understand thoroughly the role of an individual Aib residue in the peptide, the Aib residue was systematically replaced by

Ala at positions 3, 4, 6 and 13. Despite a few differences, almost all single Aib substituted AmpA analogues behaved similarly to AmpA with respect to the CD profiles. The calculated helical fractions were slightly enhanced for [Ala^3]AmpA (**15**) and [Ala^4]AmpA (**16**) in all environments under investigation, accompanied by an increase of the *R* ratios, especially in detergent micelles (see Table 2). In contrast, [Ala^{13}]AmpA (**18**) displaying a lower *R* ratio (0.93) in detergent micelles, seemed to adopt a less helical structure (0.61). Interestingly, most of single Aib-Ala substituted analogues, including the natural ones, resembled AmpA with respect to the biological activities, except for [Ala^6]AmpA (**17**) missing the hypothermic effect and AmpC (containing Ala at position 9 instead of Aib) displaying only weak activity.

Replacement of Aib at position 4 with a more conformationally constrained amino acid residue Ac_6c, belonging to the family of cyclic $C^{\alpha,\alpha}$-disubstituted glycines, (analogue [Ac_6c^4]AmpA - **20**) did not considerably influence the peptide conformation in all studied environments, but reduced the pigment induction (see Table 2). To probe the effect of Ac_6c at more sensitive positions of the sequence, where the replacement of Aib by Ala reduced or destroyed the biological activities, two analogues [$Ala^{3,8,13}$, Ac_6c^6]AmpA (**21**) and [$Ala^{3,8,13}$, Ac_6c^9]AmpA (**22**) with Ac_6c at position 6 or position 9 instead of Aib were synthesized. Compared with AmpA, the CD spectra of **21** and **22** showed higher ellipticities due to the replacement of three Aib residues by Ala. In addition, in both detergent micelles, **21** displayed lower *R* values (0.92–0.93) accompanied by lower helicities (0.60), whereas **22** was found to be more similar to AmpA.

Examining the biological activities of AmpA analogues, it was found that there was no total agreement between the pigment induction and hypothermic effect. Both activities require the presence of an aromatic amino acid at the *N*-terminus, Leu side chains, and a certain number of Aib residues. However, the pigment induction accepts a wide range of conformational flexibility, while the hypothermic effect seems to be less tolerant, judged by variations in the helical content and the *R* values. Indeed, analogues exhibiting strong pigment induction adopted a 48%–74% helical structure and the signal of peptide association (*R* value > 1) in detergent micelles was not necessary. Regarding the analogues producing a strong hypothermic response, the helical content and *R* value in detergent micelles varied in the range 60%–74% and 0.92–1.13, respectively, so that the analogues with a low *R* value adopted low helicity, as well. This suggests that there was some relationship between helicity or peptide length and the association degree in the analogues active in hypothermia. It is likely that the interaction of the peptide with the membrane followed by its self-association was necessary for the hypothermic effect. These conditions are necessary for pore formation, but might be not sufficient for ion transport. In addition, due to the absence of experimental data on the membrane modifying activities of the analogues, it is difficult to explain why some analogues (single Aib substituted analogues) displayed similar CD spectra, but exhibited biological activities in different amplitudes. Furthermore, some analogues (Leu substituted analogues) showed different CD profiles in membrane mimetic environments but were comparable in biological activities.

CONCLUSIONS

The present study, comparing the CD spectra of AmpA and its crystal structure, proposes an appropriate method of helicity estimation for Aib-rich-AmpA analogues. Subsequently, it provides the overall conformational flexibility of AmpA analogues in different environments, including membrane mimetic solvents, with an attempt to differentiate active compounds from the inactive ones. Four naturally occurring ampullosporins and their 22 synthetic analogues showed CD spectra characteristic of helical structure in organic solvents (MeCN and TFE) and detergent micelles (SDS and DPC). All analogues displayed similar CD curve shapes in organic solvents with the ratio between two negative band intensities $R < 1$. In MeCN, most of the analogues adopted a 70%–85% helical structure, which is higher than the average of 40%–60% obtained in TFE. In detergent micelles, the analogues showed different CD profiles. Some (analogues of group 1) displayed CD spectra similar to those in TFE, while the others (analogues of group 2) showed spectra with increased helicity and *R* ratio > 1. These two features indicate the interaction between the peptide and the membrane mimetic solvents as well as the helix association. Almost all inactive compounds belong to group 1, i.e. display a *R* value much less than 1. Compounds producing strong hypothermia belong to group 2, which show CD spectra in detergent micelles with helicity and *R* ratio ranging from 60% to 74% and from 0.92 to 1.13, respectively. This suggests that the interaction of the peptide with the

membrane and peptide self-association may play a role in their hypothermic effect. Although many compounds active in pigment induction share common features in CD spectra with group 2 too, there was no total agreement between the pigment induction and hypothermic effect. Since the neuroleptic effect of a compound is usually related to its capability to regulate dopamine neurotransmission in the central nervous system through its interaction with one or several membrane receptors, the biological activities of AmpA and its active analogues might result from a more complex action mechanism than from their pore forming potential. Our further research will focus on the affinity of AmpA analogues to concerned receptors. Simultaneously, the membrane modifying activity of all analogues should be screened to determine its role in their biological activities.

Acknowledgements

We thank Professor A. Ulrich's group for providing the spectropolarimeter and technical assistance and Dr A. Schlegel and Dr A. Härtl for biological activity testing. This work was supported by the Deutsche Forschungsgemeinschaft (Re 853/7-1).

REFERENCES

1. Ritzau M, Heinze S, Dornberger K, Berg A, Fleck W, Schlegel B, Härtl A, Gräfe U. Ampullosporin, a new peptaibol-type antibiotic from *Sepedonium ampullosporum* HKI-0053 with neuroleptic activity in mice. *J. Antibiotics* 1997; **50**: 722–728.
2. Kronen M, Kleinwächter P, Schlegel B, Härtl A, Gräfe U. Ampullosporins B, C, D, E_1, E_2, E_3 and E_4 from *Sepedonium ampullosporum* HKI-0053: structures and biological activities. *J. Antibiotics* 2001; **54**: 175–178.
3. Rebuffat S, Goulard C, Bodo B, Roquebert MF. The peptaibol antibiotics from *Trichoderma* soil fungi: structural diversity and membrane properties. *Recent Res. Devel. Org. Bioorg. Chem.* 1999; **3**: 65–91.
4. Chugh JK, Wallace BA. Peptaibols: models for ion channels. *Biochem. Soc. Trans.* 2001; **29**: 565–570.
5. Duclohier H, Wroblewski H. Voltage-dependent pore formation and antimicrobial activity by alamethicin and analogues. *J. Membrane Biol.* 2001; **184**: 1–12.
6. Ander R, Ohlenschläger O, Soskic V, Wenschuh H, Heise B, Brown LR. The NMR solution structure of the ion channel peptaibol chrysospermin C bound to dodecylphosphocholine micelles. *Eur. J. Biochem.* 2000; **267**: 1784–1794.
7. Snook CF, Wooley GA, Oliva G, Pattabhi V, Wood SP, Blundell TL, Wallace BA. The structure and function of antioamoebin I, a proline-rich membrane-active polypeptide. *Structure* 1998; **6**: 783–792.
8. Epand RF, Epand RM, Monaco V, Stoia S, Formaggio F, Crisma M, Toniolo C. The antimicrobial peptide trichogin and its interaction with phospholipid membranes. *Eur. J. Biochem.* 1999; **266**: 1021–1028.
9. Yau WM, William CW, Gawrisch K, Stephen HW. The preference of tryptophan for membrane interface. *Biochemistry* 1998; **37**: 14 713–14 718.
10. Popot LJ, Engelman MD. Helical membrane protein folding, stability, and evolution. *Ann. Rev. Biochem.* 2000; **69**: 881–992.
11. Grigoriev PA, Berg A, Schlegel B, Gräfe U. Differences in ion permeability of an artificial bilayer membrane caused by ampullosporin and bergofungin, new 15-membered peptaibol-type antibiotics. *Bioelectrochem. Bioenerg.* 1997; **44**: 155–158.
12. Grigoriev PA, Kronen M, Schlegel B, Härtl A, Gräfe U. Differences in ion-channel formation by ampullosporins B, C, D, and semisynthetic desacetyltryptophanyl ampullosporin A. *Bioelectrochem.* 2002; **57**: 119–121.
13. Kronen M, Görls H, Nguyen HH, Reissmann S, Bohl M, Sühnel J, Gräfe U. Crystal structure and conformational analysis of ampullosporin A. *J. Pept. Sci.* 2003; **9**: 729–744.
14. Fox OR, Richard MF. A voltage-gated ion channel model inferred from the crystal structure of alamethicin at 1.5-Å resolution. *Nature* 1982; **300**: 325–330.
15. Menestrina G, Voges KP, Jung G, Boheim G. Voltage-dependent channel formation by rods of helical polypeptides. *J. Membrane Biol.* 1986; **93**: 111–132.
16. Härtl A, Schlegel B, Dornberger K, Hülsmann H, Heinze S, Degenkolb T, Greksch G, Gräfe U. Ampullosporin, a new microbial lead structure with neuroleptic activity from *Sepedonium ampullosporum*. Poster presentation, Symposium on *Biotechnology of Natural Products*, San Diego, 1999.
17. Nguyen HH, Imhof D, Kronen M, Schlegel B, Härtl A, Gräfe U, Reissmann S. Synthesis and biological evaluation of analogues of the peptaibol ampullosporin A. *J. Med. Chem.* 2002; **45**: 2781–2787.
18. Mao D, Wachter E, Wallace BA. Folding of the mitochondrial proton adenosinetriphosphatase proteolipid channel in phospholipid vesicles. *Biochemistry* 1982; **21**: 4960–4968.
19. Greenfield NJ. Methods to estimate the conformation of proteins and polypeptides from circular dichroism data. *Anal. Biochem.* 1996; **235**: 1–10.
20. Curtis Johnson W Jr. Protein secondary structure and circular dichroism: a practical guide. *Prot. Struct. Func. Gen.* 1990; **7**: 205–214.
21. Rohl CA, Baldwin RL. Comparison of NH exchange and circular dichroism as techniques for measuring

the parameters of helix-coil transition in peptides. *Biochemistry* 1997; **36**: 8435–8442.
22. Hong DP, Hoshino M, Kuboi R, Goto Y. Clustering of fluorine-substituted alcohols as a factor responsible for their marked effects on proteins and peptides. *J. Am. Chem. Soc.* 1999; **121**: 8427–8433.
23. Gast K, Siemer A, Zirwer D, Damaschun G. Fluoroalcohol-induced structural changes of proteins: some aspects of cosolvent–protein interactions. *Eur. Biophys. J.* 2001; **30**: 273–283.
24. Reichardt C. *Solvents and Solvent Effect in Organic Chemistry*. Verlag Chemie Weinheim: New York, 1979.
25. Toniolo C, Benedetti E. The polypeptide 3_{10} helix. *TIPS* 1991; **16**: 350–353.
26. Manning M, Woody RW. Theoretical CD studies of polypeptide helices: examination of important electronic and geometric factors. *Biopolymers* 1991; **31**: 569–586.
27. Toniolo C, Polese A, Formaggio F, Crisma M, Kamphuis J. Circular dichroism spectrum of a peptide 3_{10}-helix. *J. Am. Chem. Soc.* 1996; **118**: 2744–2745.
28. Chou PY, Fasman GD. β-turns in proteins. *J. Mol. Biol.* 1977; **115**: 135–175.
29. Woody RW. Circular dichroism. *Methods Enzymol.* 1995; **246**: 34–71.
30. Chang CT, Wu CSC, Yang JT. Circular dichroism analysis of protein conformation: inclusion of β-turns. *Anal. Biochem.* 1978; **91**: 13–31.
31. Jung G, Dubischar N, Leibfritz D. Conformational changes of alamethicin induced by solvent and temperature. A 13C-NMR and circular dichroism study. *Eur. J. Biochem.* 1975; **54**: 395–409.
32. Mayr W, Oekonomopulos R, Jung G. Synthesis and conformation of a polyoxyethylene bound undecapeptide of the alamethicin helix and (2-methylalanyl-L-alanine)$_{1-7}$. *Biopolymers* 1979; **18**: 425–450.
33. Schmitt H, Winter W, Bosch R, Jung G. The α-helical conformation of the undecapeptide Boc-L-Ala-[Aib-Ala]$_2$-Glu(OBzl)-Ala-[Aib-Ala]$_2$-OMe: Synthesis, x-ray crystal structure, and conformation in solution. *Liebigs Ann. Chem.* 1982; 1304–1321.
34. Blondelle SE, Lohner K, Aguilar MI. Lipid-induced conformation and lipid-binding properties of cytolytic and antimicrobial peptides: determination and biological specificity. *BBA.* 1999; **1462**: 89–108.
35. Park K, Perczel A, Fasman DG. Differentiation between transmembrane helices and peripheral helices by the deconvolution of circular dichroism spectra of membrane protein. *Protein Sci.* 1992; **1**: 1032–1049.
36. Cascio M, Wallace BA. Conformation of alamethicin in phospholipid vesicles: implications for insertion models. *Prot. Struct. Func. Gen.* 1988; **4**: 89–98.
37. Wooley A, Wallace BA. Temperature dependence of the interaction of alamethicin helices in membranes. *Biochemistry* 1993; **32**: 9819–9825.
38. Brachais L, Mayer C, Davoust D, Molle G. Influence of secondary structure on the pore forming properties of synthetic alamethicin analogs: NMR and molecular modelling studies. *J. Pept. Sci.* 1998; **4**: 344–354.
39. Hara T, Kodama H, Higashimoto Y, Yamaguchi H, Jelokhani-Niaraki M, Ehara T, Kondo M. Side chain effect on ion channel characters of Aib rich peptides. *J. Biochem.* 2001; **130**: 749–755.
40. Lau SYM, Taneja AK, Hodges RS. Synthesis of a model protein of defined secondary and quaternary structure. *J. Biol. Chem.* 1984; **259**: 13 253–13 261.
41. Cooper TM, Woody RW. The effect of conformation on the CD of interacting helices: A theoretical study of tropomyosin. *Biopolymers* 1990; **30**: 657–676.
42. Zhou FX, Merianos HJ, Brunger AT, Engelman DM. Polar residues drive association of polyleucine transmembrane helices. *PNAS* 2001; **98**: 2250–2255.
43. Doig AJ, Baldwin RL. *N*- and *C*-capping preferences for all 20 amino acids in α-helical peptides. *Protein Sci.* 1995; **4**: 1325–1336.
44. Rohl CA, Chakrabartty A, Baldwin RL. Helix propagation and *N*-cap propensities of the amino acids measured in alanine-based peptides in 40 volume percent trifluoroethanol. *Protein Sci.* 1996; **5**: 2623–2637.
45. Doig AJ, Macarthur MW, Stapley BJ, Thornton JM. Structures of *N*-termini of helices in proteins. *Protein Sci.* 1997; **6**: 147–155.

